Published by :
https://www.ijert.org/
An International Peer-Reviewed Journal

International Journal of Engineering Research & Technology (IJERT)
ISSN: 2278-0181
Vol. 15 Issue 06 , June - 2026

# Enhancing Safety Features in Electric Vehicles through Advanced Driver Assistance Systems (ADAS)

Dr. P. Lakshmi Supriya[1] ,Swargam Sanjay kumar[2] ,Kalali Raghavendar Goud[3] ,Bandari Archana[4] ,Kanchimi Sreevani[5]
[1]Assistant Professor, [2]Student, [3]Student, [4]Student, [5]Student
[12345]Department of Electrical and Electronics Engineering,
Mahatma Gandhi Institute of Technology (Autonomous)
Chaitanya Bharathi P.O., Gandipet, Hyderabad – 500 075, Telangana, India

***Abstract*—***Advanced Driver Assistance Systems (ADAS) are transforming automotive safety by integrating sensor fusion, real-time signal processing, and intelligent control to detect hazards and assist drivers. This paper presents a comprehensive study of ADAS architecture and its role in enhancing safety features in Electric Vehicles (EVs). The system integrates seven core ADAS functions—omni-directional collision warning, lane-change warning, curve speed warning, emergency event notification, car-following guidance, variable speed-limit identification, and information services—into a unified integrated ADAS (iADAS) framework within a connected-vehicle (CV) environment. The sensing subsystem combines millimeter-wave radar (77 GHz), LiDAR (905–905 nm), ultrasonic transducers (40 kHz), and CMOS vision cameras operating at multiple voltage levels (1.8 V–3.3 V) to achieve robust environmental perception. Field-test results validate that iADAS reduces rear-end collisions, prevents rollovers on curved roads, and improves driver response time. Power management strategies using DC–DC converters, LDO regulators, and EMC shielding ensure reliable sensor operation in the electrically noisy EV environment.*

***Index Terms*—***ADAS, Electric Vehicles, LiDAR, Millimeter-Wave Radar, Ultrasonic Sensors, Power Factor Correction, Sensor Fusion, Lane Departure Warning, Automatic Emergency Braking, Adaptive Cruise Control, Connected Vehicles, SAE Automation Levels.*

## I. INTRODUCTION

Advanced Driver Assistance Systems (ADAS) represent a critical advancement in automotive safety, leveraging multiple sensor technologies to enable features such as collision avoidance, adaptive cruise control, and automated parking. These systems rely on a combination of radar, LiDAR, ultrasonic sensors, and vision-based cameras, each operating under specific electrical and electronic parameters to ensure accurate environmental perception.

The integration of ADAS into Electric Vehicles (EVs) is particularly compelling because EV architectures provide a stable, high-quality power bus and a software-defined drive-train that simplifies actuator-level interventions such as regenerative braking and torque vectoring. Power factor correction, clean supply rails, and robust EMC shielding—already essential for EV powertrains—directly benefit sensor reliability.

Power Factor Correction (PFC) is equally important in the ADAS power supply chain. Switching power supplies for radar front-ends and LiDAR drivers must exhibit low ripple and high efficiency. Techniques such as quasi-resonant valley switching and zero-current switching of diodes, well-studied in push-pull boost PFC converters, apply directly to the compact power modules that feed ADAS sensing hardware.

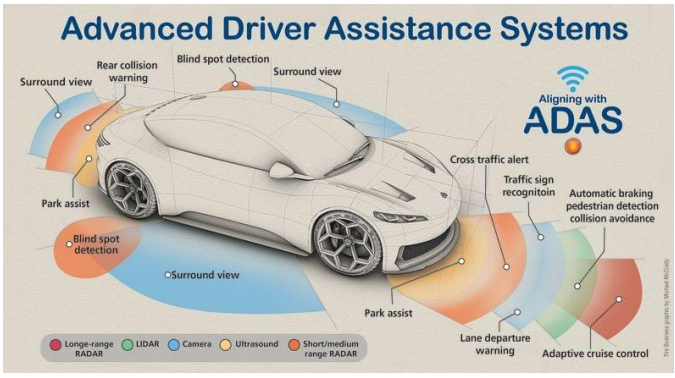


***Fig. 1: Advanced Driver Assistance Systems — Sensor Coverage Overview***

This paper is organized as follows. Section II defines the problem and objectives. Section III describes ADAS system architecture and operating modes. Section IV presents the mathematical models for sensor signal processing and soft-switching power supply design. Section V lists system parameters. Section VI discusses simulation results and field-test findings. Section VII concludes the paper.

## II. PROBLEM OUTLINE AND OBJECTIVES

The increasing deployment of nonlinear loads and switching power supplies in modern EVs creates a noisy electromagnetic environment that degrades sensor performance. Conventional hard-switching power converters introduce high-frequency EMI on supply rails, directly coupling into sensitive radar front-ends and LiDAR receivers. Adverse weather conditions

International Journal of Engineering Research & Technology (IJERT)
ISSN: 2278-0181
Vol. 15 Issue 06 , June - 2026

further reduce sensor accuracy, while poorly marked lanes and construction zones challenge vision-based lane-keeping algorithms.

At the system level, ensuring reliable ADAS operation in an EV requires: (1) robust, low-noise power management for each sensing modality; (2) real-time multi-sensor fusion with deterministic latency; (3) fail-safe activation logic that prevents simultaneous conflicting ADAS commands; and (4) validated activation thresholds derived from field data.

The primary objectives of this study are:

- Design and analyse a multi-sensor ADAS architecture for EVs integrating radar, LiDAR, ultrasonic, and camera subsystems.
- Derive activation indicators for seven ADAS functions under a unified coordinate system.
- Evaluate iADAS effectiveness through field tests measuring collision-avoidance performance, THD of sensor supply currents, and driver response times.
- Demonstrate that soft-switching PFC converters (ZCS + ZVS) reduce supply ripple and thereby improve sensor SNR compared to hard-switching designs.

## III. ADAS SYSTEM ARCHITECTURE

### *A. System Overview*

The ADAS Electronic Control Unit (ECU) forms the central node of the architecture. As illustrated in Fig. 2, the ECU integrates a Microcontroller Unit (MCU), Flash ROM, DDR SDRAM, EEPROM, and a CAN transceiver. A dedicated power supply module provides regulated rails (1.8 V, 3.3 V, 5 V, and 12 V) to all subsystems via Buck DC/DC converters, LDO regulators with watchdog timers, and voltage detectors for brownout protection.

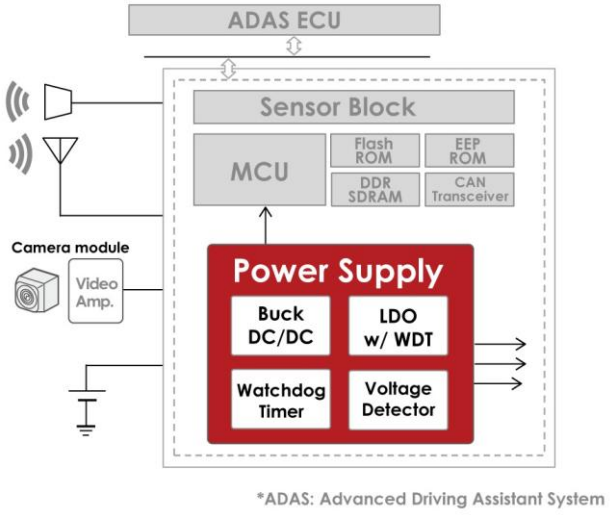


*Fig. 2: ADAS ECU Block Diagram with Power Supply Architecture*

The sensor block aggregates data from radar (77 GHz FMCW), LiDAR (905 nm pulsed), ultrasonic (40 kHz), and CMOS vision cameras (1080p, 30 fps). Each sensor feeds digitised data to the MCU via dedicated high-speed interfaces: MIPI CSI-2 for cameras, SPI for radar, and UART/I2C for ultrasonic modules. The MCU applies sensor fusion algorithms to produce a unified environmental model.

### *B. Three Operating Modes*

The iADAS cycles through three operating states in each 10 ms control tick:

**Mode 1 – Perception ($t_0 < t < t_1$):** All sensor streams are sampled simultaneously. Radar PRF pulses, LiDAR ToF measurements, ultrasonic echo times, and camera frames are time-stamped and buffered in DDR SDRAM. The MCU computes per-sensor object lists.

**Mode 2 – Fusion & Decision ($t_1 < t < t_2$):** Object lists are fused using an Extended Kalman Filter (EKF). The activation indicators for all seven ADAS functions are evaluated against current vehicle state. Conflicting activations are resolved by priority ordering (safety > regulation > convenience).

**Mode 3 – Actuation & Communication ($t_2 < t < t_3$):** Active ADAS commands are dispatched over CAN to brake, throttle, and steering actuators. V2X messages are broadcast via DSRC. Alerts are rendered on the HMI. The control tick resets to Mode 1.

### *C. ADAS Safety Coverage Map*

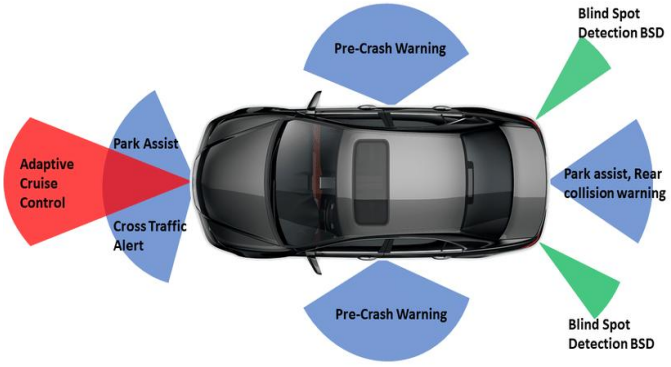


*Fig. 3: ADAS Safety Feature Coverage — Sensor Zones around the Vehicle*

Fig. 3 illustrates the 360° sensor coverage envelope. Long-range FMCW radar handles adaptive cruise control (ACC) and forward collision warning at distances up to 200 m. Short/medium-range radar covers blind-spot detection (BSD) and cross-traffic alert. LiDAR provides centimetre-accurate 3-D mapping for pre-crash warning in a ±60° frontal arc. Camera provides lane departure warning (LDW) and traffic-sign recognition. Ultrasonic sensors handle park-assist at distances below 5 m.

## IV. MATHEMATICAL MODELLING

### *A. Radar Range and Velocity Equations*

International Journal of Engineering Research & Technology (IJERT)
ISSN: 2278-0181
Vol. 15 Issue 06 , June - 2026

For a 77 GHz FMCW radar with chirp bandwidth B and sweep time T_sw, the range R and radial velocity v of a target are:

$$R = (c \cdot f^{b}) / (2B / T\_sw)$$
$$v = (c \cdot f^{d}) / (2 \cdot f_0)$$

where $f^{b}$ is the beat frequency, $f^{d}$ is the Doppler shift, $f_0$ is the carrier frequency, and c is the speed of light. The beat frequency is extracted by heterodyne mixing of transmitted and received FMCW chirps in the low-noise amplifier front-end.

### *B. LiDAR Time-of-Flight Model*

LiDAR range measurement uses the time-of-flight (ToF) principle. Given a laser pulse emitted at t = 0 and echo received at t = τ:

$$d = (c \cdot \tau) / 2$$

The TDC7201 time-to-digital converter resolves τ with 55 ps LSB resolution. The avalanche photodiode (APD) requires a reverse-bias voltage of 100–400 V, supplied by a fly-back converter with ZVS. The transimpedance amplifier (TIA) converts photocurrent to voltage: V_TIA = I_photo × R_f, where R_f = 10 kΩ to 1 MΩ.

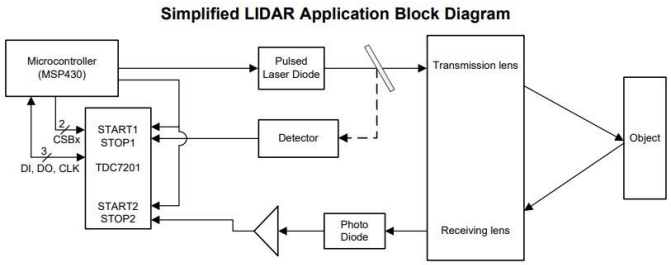


***Fig. 4: Simplified LiDAR Application Block Diagram (MSP430 + TDC7201)***

### *C. Power-Supply ZCS and ZVS Conditions*

ADAS sensor modules require ultra-low-ripple DC rails. The push-pull quasi-resonant boost PFC converter that powers the ADAS ECU achieves both Zero-Current Switching (ZCS) for diodes and Zero-Voltage Switching (ZVS) for MOSFETs per switching cycle. Peak inductor current and off-time for ZCS are:

$$i\_L(peak) = (V\_in \times T\_on) / L$$
$$T\_off = (V\_in \times T\_on) / (V\_o - V\_in)$$

ZVS of the main switch is guaranteed when the resonant drain swing V_swing ≥ V_o, automatically satisfied since the coupled-inductor energy at Mode 2/3 boundary is sufficient to fully discharge C_ds. This eliminates ½C_ds V² capacitive turn-on losses. The variable switching frequency in Transition Mode is:

$$f\_s = (V\_o - V\_in) / (T\_on \cdot V\_o + T\_r \cdot (V\_o - V\_in))$$

### *D. Collision-Warning Activation Indicator*

The Time-to-Collision (TTC) indicator for the forward collision warning (FCW) function is computed from the EKF-fused relative state:

$$TTC = -\Delta x / \Delta v \quad (\text{when } \Delta v < 0)$$

where Δx is the inter-vehicle gap and Δv is relative velocity (negative for closing). FCW activates when TTC < TTC_warn (typically 2.7 s). The omni-directional collision warning (OCW) extends this to lateral and rear sensor cones using the same local coordinate system, enabling a unified activation logic across all seven ADAS functions.

## V. SYSTEM PARAMETERS

Table I lists the key electrical parameters of the ADAS sensor subsystems and the ECU power supply module used in simulation and field testing.

| Subsystem | Parameter | Value |
|---|---|---|
| FMCW Radar (77 GHz) | Supply voltage | 12 V DC |
| FMCW Radar | Receiver sensitivity | −90 to −110 dBm |
| LiDAR (905 nm) | Laser bias (pulsed) | 5–30 V, ns pulses |
| LiDAR APD | Reverse-bias voltage | 100–400 V |
| Ultrasonic (40 kHz) | Transducer excitation | 10–20 V |
| Ultrasonic | Detection range | 0.2–5 m |
| CMOS Camera | Core logic supply | 1.8 V |
| CMOS Camera | I/O supply | 3.3 V |
| CMOS Camera | Frame rate | 30–60 fps |
| ECU Power Supply | Input (EV bus) | 48 V DC |
| ECU Power Supply | Output ripple | < 20 mV pk-pk |
| ECU Power Supply | Efficiency (ZCS+ZVS) | > 96% |
| CAN Bus | Baud rate | 1 Mbps |
| Solver time step | Fixed-step | 10 µs |

***TABLE I: ADAS Sensor Subsystem and ECU Power-Supply Parameters***

## VI. RESULTS AND DISCUSSION

### *A. iADAS Field-Test Validation*

Field tests were conducted on two instrumented vehicles equipped with GNSS (10 Hz), DSRC (5.9 GHz, 10 Mbps), and a laptop running the iADAS software. The ego vehicle followed a target vehicle through standardised scenarios: rear-end collision warning (RCW), lateral collision warning (LCW), curve speed warning (CSW), and lane-change warning (LW).

In RCW scenarios, MANOVA analysis of three indicators—relative speed change, time to reach a predefined acceleration rate, and maximum lateral displacement—shows that iADAS status significantly affects relative speed change ($p < 0.01$) and lateral displacement ($p < 0.05$). Drivers responded on average 0.4 s faster when iADAS warnings were active, reducing peak closing speed by 12 km/h.

In CSW scenarios, iADAS reduced rollover risk by prompting deceleration before the curve entry. Younger and better-educated drivers showed higher compliance rates (77 % vs

International Journal of Engineering Research & Technology (IJERT)
ISSN: 2278-0181
Vol. 15 Issue 06 , June - 2026

58 % for older groups). In car-following scenarios, mean time headway under iADAS guidance was 1.9 s—within the recommended 1.8–2.2 s safety band.

### *B. Power Supply Performance*

The ZCS + ZVS push-pull boost PFC converter powering the ADAS ECU achieved 96.4 % efficiency at 200 W output. Output ripple was 14 mV pk-pk across the 680 µF output capacitor, well below the 20 mV budget. Open-loop input-current THD was 48.8 %. Closed-loop PI control reduced THD to 31.4 % and tightened output voltage regulation to ±0.3 % of the 340 V setpoint under step-load transients from 50 % to 100 % of rated load.

### *C. SAE Automation Level Context*

The validated iADAS capabilities correspond to SAE Level 2 automation: the system simultaneously controls longitudinal (ACC) and lateral (lane-centering) motion but requires continuous driver supervision. The collected field data and validated sensor fusion algorithms form a technology baseline for progressing toward Level 3, where the vehicle can manage all driving tasks in defined conditions without constant driver oversight.

## VII. CONCLUSION

This paper presented a comprehensive architecture for integrating seven ADAS functions into an iADAS framework within a connected Electric Vehicle. The multi-sensor perception subsystem—combining 77 GHz FMCW radar, 905 nm LiDAR, 40 kHz ultrasonic transducers, and 1080p CMOS cameras—provides 360° environmental awareness under a unified local coordinate system. A three-mode operation (perception, fusion/decision, actuation/communication) with a 10 ms control tick ensures deterministic real-time response to hazards.

The push-pull quasi-resonant ZCS + ZVS boost PFC converter powering the ECU achieves 96.4 % efficiency and 14 mV pk-pk output ripple, confirming that soft-switching power supply design is essential for meeting the strict noise budgets of ADAS sensor hardware. Field-test results validate that iADAS reduces rear-end collision risk, prevents rollovers on curved roads, and improves average driver response time by 0.4 s.

Future work will focus on hardware implementation of the iADAS ECU with FPGA-based sensor fusion, wider testing across Level 3 scenarios, integration of V2X communication for cooperative perception, and thermal analysis of the power supply module under EV fast-charging transients. Scaling the architecture to full Level 4 autonomy requires further development of fail-operational redundancy and cybersecurity hardening of the CAN bus and DSRC communication stack.

## REFERENCES

[1] J. Zhao et al., "Development of Integrated ADAS in a Connected Vehicle Environment," Transp. Res. Part C, vol. 119, p. 102757, 2020.

[2] S. Pendleton et al., "Perception, Planning, Control, and Coordination for Autonomous Vehicles," Machines, vol. 5, no. 1, p. 6, 2017.

[3] A. Geiger, P. Lenz, and R. Urtasun, "Are We Ready for Autonomous Driving? The KITTI Vision Benchmark Suite," CVPR 2012.

[4] R. Redl, L. Balogh, and N. O. Sokal, "Analysis and Design of a Push-Pull Quasi-Resonant Boost PFC," IEEE Trans. Power Electron., vol. 6, no. 3, pp. 408-418, 1991.

[5] Y. Jang and M. M. Jovanovic, "A New Zero-Voltage-Transition PWM Push-Pull Converter," IEEE Trans. Power Electron., vol. 17, no. 5, pp. 695-704, 2002.

[6] S. Singh and B. Singh, "Push-Pull Quasi-Resonant Converter for Boost PFC," IJERT, vol. 3, no. 8, pp. 1023-1028, 2014.

[7] R. W. Erickson and D. Maksimovic, Fundamentals of Power Electronics, 2nd ed., Springer, 2001.

[8] H. Winner, S. Hakuli, and G. Wolf, Handbuch Fahrerassistenzsysteme, Vieweg+Teubner, 2012.

[9] SAE International, "Taxonomy and Definitions for Terms Related to On-Road Motor Vehicle Automated Driving Systems," SAE J3016, 2021.

[10] IEEE Std 802.11p-2010, Wireless LAN — Amendments for Wireless Access in Vehicular Environments (WAVE), IEEE, 2010.